

# Application of physical modelling of debris flow triggering to field conditions: Limitations posed by boundary conditions

Harry M. Blijenberg \*

*Statistics Netherlands, Division of Macro-economic Statistics and Dissemination, PO Box 4000, 2270 JM Voorburg, The Netherlands*

Accepted 11 December 2006

Available online 20 January 2007

## Abstract

Debris flows are often triggered by Hortonian overland flow during high-intensity rainstorms. Data derived from debris flow trigger zones in the southern French Alps were fed into a physical model of debris flow triggering based on Takahashi. Using a Monte Carlo approach with 1000 runs, the results show a wide distribution of safety factor values, indicating that physical modelling based on actual field measurements may not always be practical.

As all safety factor values obtained are well below 1 even though debris flows only occur during very high-intensity rainstorms, the model used must be inappropriate. Apparently, the composition of the overland flow plays an important role: during high-intensity rainstorms it usually has a very high sediment content and contains stones. This prevents it from flowing through the pores of coarse debris accumulations in the central gully of a trigger zone; it will rather run over the debris. This situation is more stable than with the fluid flowing through the pores. The behaviour switch of the fluid above a certain sediment and stone content thus drastically changes the triggering conditions for debris flows and it is concluded that debris flow triggering in the area requires the occurrence of both overland flow and landsliding.

© 2007 Elsevier B.V. All rights reserved.

*Keywords:* Debris flow; Runoff; Sediment content; Viscosity; Stability; Physical modelling; Uncertainty modelling

## 1. Introduction

Debris flows are mass movements consisting of granular solids, water and air moving as a viscous flow (Varnes, 1978). They have been reported from mountainous areas all over the world (e.g. Pierson, 1981; Kotarba, 1997; Sassa et al., 1997). Because of their high velocities, usually in the order of several metres per second, they are one of the most dangerous types of mass movement and cause significant economic losses as well as casualties (Martinez et al., 1995). With the increasing use of natural

resources in remote areas, the economic significance of damage by debris flows is likely to increase.

The study of debris flows is hampered by the inaccessibility of their trigger zones. Not only are such trigger zones often difficult to access, usually they are also subject to other active processes such as rock fall (Blijenberg, 1998). As a result, debris flows have long received less attention from the scientific community than landslides, especially field studies. Debris flow studies have mainly dealt with laboratory simulations (Bagnold, 1954; Van Steijn and Coutard, 1989), modelling trigger and movement mechanisms (Takahashi, 1978, 1981), deposits (Innes, 1985; Strunk, 1991) and case studies of extreme events that caused damage

\* Tel.: +31 06 28 11 29 89.

E-mail address: [h.m.blijenberg@hccnet.nl](mailto:h.m.blijenberg@hccnet.nl).

or casualties (Campbell, 1974; Haeberli et al., 1990; Zimmermann, 1990; Lahousse and Salvador, 1998; Lin and Jeng, 2000; Villi and Dal Pra, 2002).

Modelling the triggering and motion of debris flows has both practical and scientific interests. From a practical viewpoint, risk areas may be identified where no building will take place or evacuation plans may be developed in the case of a built-up area. Also, critical conditions for triggering debris flows can be identified and monitored, and early-warning systems may be based on these. Ideally, modelling debris flow triggering should be based on a physical, and therefore generally applicable, model. Rainfall, soil and terrain data obtained from field measurements should be fed into such a model in order to forecast the critical conditions and frequency. However, the uncertainty in the measured values of the data to be fed into such a model makes a fully quantitative physical approach difficult (Ocakuglu et al., 2002) making a probabilistic approach necessary (Duzgun et al., 2002).

This paper discusses the application of a physical model to quantify debris flow triggering conditions using input data obtained from field measurements. The study was part of the project ‘The temporal analysis of debris flows in an alpine environment’, which was part of the EU-project ‘Temporal occurrence and forecasting of landsliding in the European Community’ (Flageollet,

1993; European Commission, 1994). It was carried out between 1991 and 1998 at Utrecht University. Field data were gathered during the period 1991–1995 in the Bachelard Valley in the southern French Alps (Fig. 1).

The paper starts with the presentation of the physical model and then proceeds with the field measurements. In the next step the data obtained are fed into the model to obtain model results. These results are discussed and finally conclusions are drawn concerning the practical use and limitations of the physical modelling approach of debris flow triggering.

## 2. Modelling debris flow triggering

Debris flows can be triggered in many ways. Landslides can transform into debris flows by dilatancy or liquefaction during movement, as described by Fleming et al. (1989), Iverson et al. (1997) and Johnson and Rahn (1970). Takahashi (1978, 1981) and Takahashi et al. (1981, 1992) describe the spontaneous triggering of a debris flow by dilatancy when a water film of a certain thickness appears at the surface of a saturated body of debris in a channel. Other triggering mechanisms include spontaneous liquefaction, damming of water behind debris dams with subsequent breaching (Costa, 1984), undrained loading (Sassa et al., 1997).

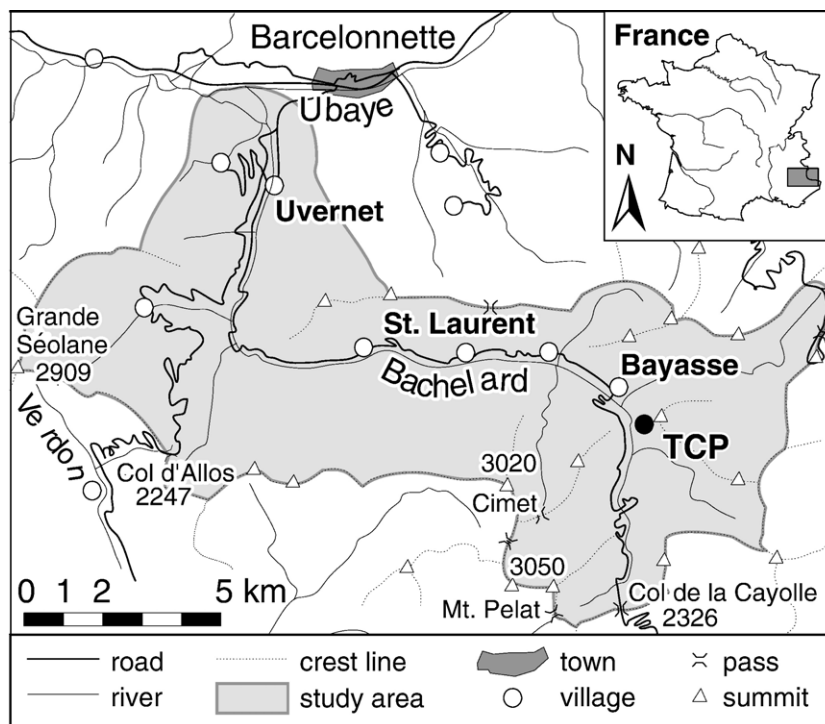


Fig. 1. Location of the study area.

Usually an increase of pore pressures caused by a supply of water to the material provides the force for triggering movement. Water is supplied by rainfall, snowmelt or a combination of both (Azimi and Desvarreux, 1974) or –less frequently– by drainage of lakes, rapid snow and ice melt during volcanic eruptions or stream diversions. External forces can also trigger the movement: vibrations from earthquakes (Martinez et al., 1995), passing debris flows or volcanic eruptions, and impact or loading forces from snow avalanches or mass movements (Sassa, 1985; Sassa et al., 1997). When long-duration rainfall of moderate intensity occurs, both the groundwater table and the water content in the soil will rise, resulting in high pore pressures. Both effects favour debris flow triggering (Kobashi and Suzuki, 1987; Zimmermann, 1990).

In the southern French Alps, most debris flows are triggered by short-duration high-intensity rainstorms: Van Asch and Van Steijn (1991) mention eye-witness observations of 50–100 mm/h rainfall during 5–10 min causing debris flow triggering. During such rainstorms, Hortonian overland flow incorporates fine-grained debris, concentrates towards a central gully in the trigger zone and enters an accumulation of loose, cohesionless, coarse debris. Depending on the fluid pressure exerted by the muddy fluid, the coarse debris may or may not be destabilized and move downslope as a debris flow.

Short-duration high-intensity rainstorms causing debris flows have also been reported by Berti et al. (1999), Cannon et al. (2001), Kotarba (1989), Okunishi et al. (1988) and Zimmermann (1990).

The model for debris flow triggering used in this paper is based on the model developed by Takahashi (1978, 1981) and Takahashi et al. (1981, 1992). Takahashi originally developed his model to describe the spontaneous transformation of debris on a gully bed into a debris flow. This happens by dilatancy as soon as a water film of a certain depth  $h_0$  appears on the surface of a saturated body of debris. Fig. 2 shows three different

situations distinguished by Takahashi. The equilibrium model used by Takahashi is based on an infinite slope model. The shear stress  $\tau$  at depth  $y$  is given by:

$$\tau = (c_*(\rho_s - \rho_f)y + \rho_f(y + h_0))g \sin \beta \tag{1}$$

and the maximum shear resistance  $\tau_f$  by:

$$\tau_f = c_*(\rho_s - \rho_f)g y \cos \beta \tan \varphi'_s \tag{2}$$

where:  $c_*$  = volumetric concentration of solids;  $\rho_s$  = solids density;  $\rho_f$  = fluid density;  $g$  = gravity acceleration,  $\beta$  = slope angle,  $\varphi'_s$  = effective static angle of internal friction.

Situation 1 in Fig. 2 shows the non-stationary bed situation, where shear stress increases faster with depth than shear resistance:

$$\frac{d\tau}{dy} > \frac{d\tau_f}{dy} \tag{3}$$

In this situation the whole bed of debris will start to move. The combination of Eqs. (1) and (2) yields the critical slope angle:

$$\tan \beta \geq \left( \frac{c_*(\rho_s - \rho_f)}{c_*(\rho_s - \rho_f) + \rho_f} \tan \varphi'_s \right) \tag{4}$$

If  $h_0 = 0$  or the body of debris is not fully saturated, failure may still occur. However, in this situation there is not enough water available for the debris to dilate and lose consistency, so a landslide is formed rather than a debris flow.

In the second and third situations in Fig. 2 the shear resistance of the debris increases faster with depth than the shear stress:

$$\frac{d\tau}{dy} < \frac{d\tau_f}{dy} \tag{5}$$

In this situation failure can only occur if  $h_0 > 0$ . At a certain depth  $y_f$  the shear stress equals the shear resistance and up to this depth failure will occur. In situation two, where  $y_f$  is below the base of the debris

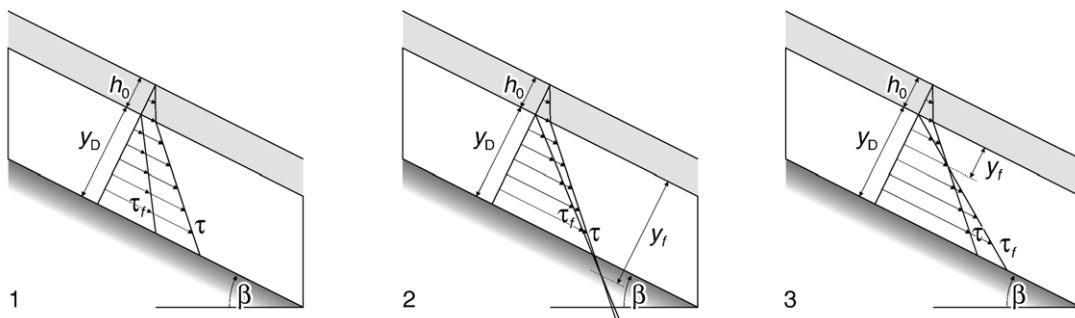


Fig. 2. Characteristic shear-strength and shear-stress distributions in saturated debris (after Takahashi, 1978, 1980).

accumulation, the limit of moving and stable material is formed by the gully floor. In the third situation, not all of the debris mass will move. This is the (quasi-) stationary bed situation. Takahashi gives an additional boundary condition for this case:

$$y_f \geq d_{ch} \quad (6)$$

where:  $d_{ch}$  = characteristic grain diameter.

For  $y_f < d_{ch}$  no debris flow can take place, only transport by streamflow. A debris flow can occur if:

$$\tan\beta \geq \frac{c_*(\rho_s - \rho_f)}{c_*(\rho_s - \rho_f) + \rho_f \left(1 + \frac{h_0}{d_{ch}}\right)} \tan\varphi'_s \quad (7)$$

One more boundary condition is introduced by Takahashi to exclude situations in which there is too much water for the debris to be uniformly dispersed throughout the depth of flow:

$$y_f \geq \kappa h_0 \quad (8)$$

Usually  $\kappa \approx 1$ . Combination of the left part of Eq. (7) with Eq. (8) gives the critical slope angle for the occurrence of debris flows:

$$\tan\beta = \frac{c_*(\rho_s - \rho_f)}{c_*(\rho_s - \rho_f) + \rho_f \left(1 + \frac{1}{\kappa}\right)} \tan\varphi'_s \quad (9)$$

This equation can also be presented in a form similar to slope stability equations. For fully saturated, cohesionless materials (Blijenberg, 1995):

$$F = \frac{\text{shear resistance } \tau_f}{\text{shear stress } \tau} = \frac{c_*(\rho_s - \rho_f)}{c_*(\rho_s - \rho_f) + \rho_f \left(1 + \frac{1}{\kappa}\right)} \frac{\tan\varphi'_s}{\tan\beta} \quad (10)$$

For realistic values ( $c_*=0.7$ ;  $\rho_s=2600 \text{ kg m}^{-3}$ ;  $\rho_f=1000 \text{ kg m}^{-3}$ ;  $\kappa=0.75$ ;  $\tan\varphi'_s=0.8$ ) debris flows may occur on slopes between  $14.5^\circ$  and  $22.9^\circ$ . On steeper slopes, landslides occur rather than debris flows. Such landslides may or may not turn into debris flows while moving.

### 3. Input data for the model

Eq. (10) was used to quantify the conditions in a typical debris flow trigger zone (location TCP in Fig. 1) in the Bachelard Valley. In order to use this model, the parameters in the equation had to be determined. Five out of the six parameters in this equation were derived from field measurements at or near TCP; the value of  $\kappa$  was fixed at 1. As data collection in the field was

hampered by difficult terrain conditions, practical considerations played an important role in deciding on which methods to use.

#### 3.1. Volumetric solids content of static, coarse debris $c_*$

The volumetric solids content of static, coarse debris  $c_*$  was measured by filling a bucket of known volume with coarse debris (no sand or smaller-sized material) and then filling the pores with water. Porosity  $\theta_s$  is calculated by dividing the volume of water in the bucket by the total volume of water and debris in the bucket, and then  $c_*$  can be calculated from its relation with porosity:  $c_*=1-\theta_s$ .

Measurements were done with samples varying in average grain size, in sorting and in packing. Stone size sorting was determined visually in the field and divided into 4 classes with increasingly wide stone size distributions: *good*, *quite poor*, *poor* and *very poor*.

Measurements of  $c_*$  did not yield unexpected results (Table 1):  $c_*$  is independent of average stone size but shows a strong relation with packing and stone size sorting. Densely packed or poorly sorted samples have higher  $c_*$  than loosely packed or well sorted ones. Field observations revealed that coarse debris in debris flow trigger zones usually has *good*, *quite poor* or *poor* sorting. Therefore in this study, a  $c_*$  distribution based on the data in these three classes was used to feed into the model:  $0.54 \pm 0.04$ .

#### 3.2. Solids density $\rho_s$

The density of different rock types was calculated from measurements of displaced water volume and weight. These showed that sandstone and flysch have solids densities  $\rho_s$  of about  $2.4\text{--}2.7 \cdot 10^3 \text{ kg m}^{-3}$ ; limestone is slightly less dense with  $2.2\text{--}2.5 \cdot 10^3 \text{ kg m}^{-3}$ . As

Table 1  
Volumetric solids content of static, coarse debris  $c_*$

Debris parameter	Subset	Number of samples	Volumetric solids content	
			Average	Standard deviation
	All samples	110	0.55	0.05
Packing	Dense	47	0.57	0.04
	Loose	57	0.52	0.04
Average grain size	10–25 mm	36	0.56	0.05
	30–50 mm	74	0.54	0.05
Grain size sorting	Good	58	0.52	0.04
	Quite poor	10	0.56	0.01
	Poor	37	0.58	0.04
	Very poor	5	0.63	0.04

there were too few measurements to obtain reliable distributions of solids densities, we have used the distribution of regolith material solids density:  $\rho_s = 2.51 \pm 0.28 \cdot 10^3 \text{ kg m}^{-3}$  ( $N=41$ ).

### 3.3. Liquid density $\rho_f$

Unfortunately, liquid density  $\rho_f$  of actual runoff could not be determined in the field. Camcorder images showed that runoff during debris flow triggering events has a very high sediment content, which we estimated to be in the order of 30–50% of the runoff volume. In fact, the runoff may already have the characteristics of a debris flow consisting of relatively fine-grained materials derived from the regolith on the side slopes of the trigger zone. Similar sediment contents have also been reported by Oostwoud Wijdenes and Ergenzinger (2003), who also noted the occurrence of miniature debris flows during their rainfall simulations on marls in Southeast France. They found sediment concentrations in these miniature debris flows of 40% and up to 54% in runoff. In the same area, Mathys et al. (2003) found sediment concentrations of up to about 30% (800 g/l) in runoff from an 86 ha large catchment. For the modelling exercise in this paper, we assume a sediment content of  $30 \pm 5\%$ , which when combined with a regolith solids density of  $2.51 \pm 0.28 \cdot 10^3 \text{ kg m}^{-3}$  results in a fluid density distribution of  $1.48 \pm 0.12 \cdot 10^3 \text{ kg m}^{-3}$ .

### 3.4. Effective static internal friction angle $\varphi'_s$

Static internal friction angles could not be determined with the simple field test described in Blijenberg (1995, 1998) because single particle effects had too much influence on initial failure. However kinetic internal friction angles could be determined with the test method and were later related to  $\varphi'_s$ .

The tests were performed on the rough, angular debris that can be found on many scree slopes in the study area: mixture 1 consists of sandstone, limestone and marl, and mixture 2 of sandstone and limestone. For both debris types, 50 tests were done and the principal axes of 100 stones were measured to derive stone size, stone shape and stone size distribution parameters. The maximum error for individual measurements was estimated to be about  $2^\circ$ .

Kinetic internal friction angles  $\varphi'_k$  for individual tests range from  $31$ – $43^\circ$ .  $\varphi'_k$ -distributions for both mixtures are normal at a 95% confidence level. The results are given in Table 2. The average  $\varphi'_k$  values range from  $36.6^\circ$  for mixture 1 to  $38.7^\circ$  for mixture 2, with standard deviations of about  $2^\circ$ .

These values are in accordance with those obtained by others. Kenney (1984) reported  $\varphi'_k$  values of  $37^\circ$  for well-graded, crushed, angular sandstone and slate with average grain sizes of about 5–40 mm and Statham (1977) found kinetic internal friction angles of  $38$ – $42^\circ$  for angular gravel and talus, slightly higher than in this study. Martins (1991) obtained results for  $\varphi'_s$  of  $38$ – $41^\circ$  for angular, 30–80 mm fragments of crushed rock. Charles (1991) mentions results on unconsolidated gravel at Megget Dam in Scotland yielding  $\varphi'_s = 37.5^\circ$  and Gregoretti (2000) found  $\varphi'_s = 41$ – $42.5^\circ$  for well-sorted fine gravel. For a sand–gravel mixture, Iverson et al. (1997) determined  $\varphi'_s = 40^\circ$ .

The large difference in  $\varphi'_k$  between the two mixtures, could be due to the presence of a small (5–10%) marl fraction in mixture 1, but it might also be the result of differences in stone size distribution. The correlation between  $\varphi'_k$  and stone size sorting and stone shape found by Blijenberg (1995, 1998) can completely explain the difference in  $\varphi'_k$  between both mixtures:

$$\varphi_{k'} = 42.81 + 1.062 \text{ cv}_v - 13.4 \text{ m}_{b/a} \quad (11)$$

Where  $\text{cv}_v$  = coefficient of variation of stone volumes and  $\text{m}_{b/a}$  = stone shape based on the intermediate to major axis ratios.

Such a relation agrees with Lambe and Whitman (1969) and Statham (1977). Average stone size probably does not have an influence on  $\varphi'_k$ , as was also concluded by Statham (1977).

Taking into account that static internal friction angles may be some  $0$ – $3^\circ$  (Martins, 1991) to  $4^\circ$  (Hungur and Morgenstern, 1984a,b) higher than kinetic internal friction angles, and that debris on scree slopes usually has a poor to good sorting,  $\varphi'_k$  values might be about  $38^\circ$  and  $\varphi'_s$  values about  $40^\circ$ . Therefore, in this study  $\varphi'_s$  is assumed to have a distribution of  $40.0 \pm 2.0^\circ$ .

### 3.5. Slope angle $\beta$

The slope angle  $\beta$  was determined in the main channel of the TCP debris flow trigger zone. The slope angle varies from about  $35^\circ$  at the lower edge

Table 2  
Kinetic internal friction angles of two coarse, cohesionless debris types

Debris type	Number of samples	Average	Standard deviation	Stone shape	Stone size distribution
				$\text{m}_{b/a}$	$\text{cv}_v$
Mixture 1	50	$36.6^\circ$	$1.8^\circ$	0.67	3
Mixture 2	50	$38.7^\circ$	$2.0^\circ$	0.67	5

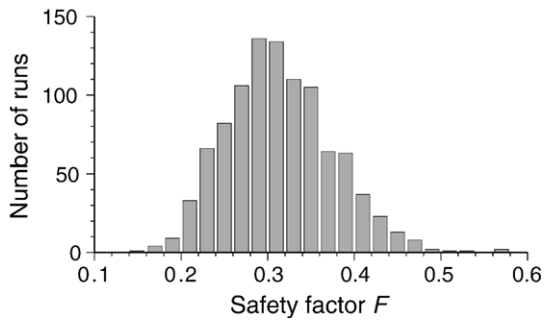


Fig. 3. Distribution of  $F$ -values from a Monte Carlo simulation of Eq. (10) (1000 runs).

of the channel to about  $38^\circ$  at the top of the scree in the channel. Debris flow triggering is assumed to take place mainly at the lower edge of the channel, even though smaller debris flow tracks have been found higher up in the main channel. Therefore, the slope angle at the lower edge of the channel is used:  $35^\circ$ .

#### 4. Model results and discussion

Eq. (10) and the values of the input parameters obtained in the previous section were used for modelling debris flow triggering conditions in the TCP debris flow trigger zone during an extreme rainfall event. A Monte Carlo simulation was run to take into account the uncertainties of the input parameters due to natural variations and measurement errors. The number of runs in the simulation was 1000 (see Fig. 3). With the assumptions of a fully saturated layer of debris and additional assumptions about the density of the runoff fluid—or more precisely the sediment content—, the relation between the static and the kinetic internal friction angle, normally distributed input parameters (other than the slope angle), and the value of  $\kappa$  ( $=1$ ), the resulting safety factor distribution is  $F=0.19\pm 0.06$ . The input parameter values used are:

$c_*$	$0.54\pm 0.04$
$\rho_s$	$2.51\pm 0.28 \cdot 10^3 \text{ kg m}^{-3}$
$\rho_f$	$1.48\pm 0.12 \cdot 10^3 \text{ kg m}^{-3}$ (at $30\pm 5\%$ sediment content)
$\varphi'_s$	$40.0\pm 2.0^\circ$
$\beta$	$35.0^\circ$

The combined effect of uncertainties in the input values of the triggering model is clearly shown in Fig. 3: the model results are much more scattered around the

mean than the values of the input parameters, as shown by the coefficient of variation in Table 3.

Conspicuously, all  $F$ -values obtained from the model runs are well below 1, indicating certain failure. However, this is not in agreement with actual debris flow triggering in the TCP debris flow trigger zone. Even when using conservative estimates for the input parameters  $\rho_f$  ( $1.09\pm 0.03 \cdot 10^3 \text{ kg m}^{-3}$  at  $4\pm 1\%$  sediment content);  $\varphi'_s$  ( $42.0\pm 2.0^\circ$ );  $\beta$  ( $30.0^\circ$ ) and  $\kappa$  ( $0.75$ ), the safety factor is well below 1:  $F=0.36\pm 0.07$ . This indicates that the assumption of a fully saturated layer must be incorrect. This also implies that the model given by Eq. (10) must be inapplicable for debris flow triggering at TCP, as saturation is a prerequisite for debris flow formation in this model. According to Takahashi (1981) failure may also occur in a non-saturated situation, but a landslide occurs rather than a debris flow. This indicates that debris flows probably develop from small landslides in the TCP debris flow trigger zone. As there is little or no direct field evidence of landslide activity, the transformation must take place immediately after initial failure of the landslide.

This hypothesis of debris flow formation is supported by other observations at TCP. The main factor is the flow behaviour of the fluid that triggers the debris flow. Camcorder images showed that sediment content of runoff can be very high during heavy rainfall and could well be 30–50%. The fluid may also contain stones. At a high sediment content, viscosity can be very high and depends strongly on small changes in sediment content, as found by Bentley (1979; see Fig. 4) and Chen (1986):

$$\eta_N = \eta_{if} \left( 1 - \frac{c_s}{c_*} \right)^{-Bc_*} \quad (12)$$

where:  $\eta_N$ =Newtonian viscosity;  $\eta_{if}$ =viscosity of interstitial fluid;  $c_s$ =volumetric solids content of debris;  $c_*$ =volumetric solids content of static debris.

According to Chen (1988),  $B$  represents an *intrinsic viscosity* of the fluid and is about 2.5 for mono-sized rigid spheres. With  $B=2.5$  and  $c_*=0.6$ , the fluid viscosity would be about 3 times higher than water at a sediment content  $c_s=0.3$ , 5 times higher than water at  $c_s=0.4$  and 15 times higher at  $c_s=0.5$ . This strongly influences the fluid flow through the pores of an

Table 3

Relative uncertainties in values as indicated by the coefficient of variation

Variable	$\kappa$	$\beta$	$\varphi'_s$	$\rho_f$	$c_*$	$\rho_s$	$F$
Coefficient of variation	0	0	0.05	0.08	0.09	0.11	0.3

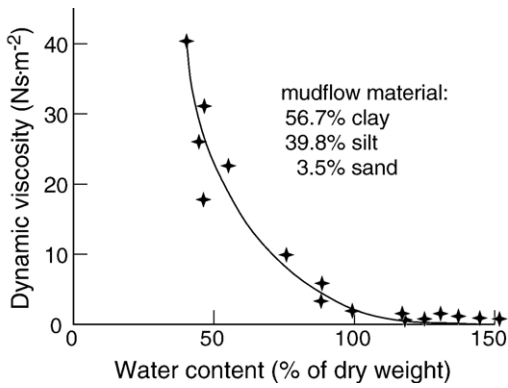


Fig. 4. Relation between viscosity and water content (after Bentley, 1979).

accumulation of coarse debris: with a high discharge of the fluid reaching the coarse debris, not all of the fluid may flow into the pores of the debris. A part may simply run over the debris. The heterogeneous composition of the fluid enhances this effect, as the stones in the fluid may effectively block pores in the debris mass.

In Fig. 5 the three typical situations are depicted when sediment-laden runoff reaches the coarse-debris accumulation on the channel floor of the debris flow trigger zone. From left to right the viscosity and stone content of the runoff fluid decrease. For each of these situations, the value of the safety factor  $F$  is calculated from an infinite slope model using the average values for each of the input parameters:  $\beta=35^\circ$ ,  $\varphi'_s=40^\circ$ ,  $c_*=0.54$ ,  $\rho_s=2510 \text{ kg m}^{-3}$  and  $\rho_f=1480 \text{ kg m}^{-3}$  and effective cohesion for the coarse debris  $c'=0 \text{ N m}^{-2}$ .

The leftmost situation represents immediate and complete clogging of the pores in the debris mass by the stones in the runoff fluid. The runoff will flow over

the surface of the coarse debris and no flow takes place within the coarse debris (Fig. 5(a)). This results in  $F=1.20$  (stable). The situation in the middle (Fig. 5(b)) occurs at a lesser viscosity and stone content. Now the fluid flows through the pores of the coarse debris, completely saturating it and resulting in  $F=0.33$  (failure). Finally, the rightmost situation (Fig. 5(c)) is for a low-viscosity fluid flowing through the coarse debris, saturating only the lower half of the debris and resulting in  $F=0.68$  (failure). It can be seen that the  $F$ -values for these situations vary by a factor 3–4. In situations (b) and (c) failure would occur, situation (a) is stable. It shows that debris flow triggering probably starts when some runoff flows through the debris mass, triggering a landslide. The remainder of the runoff, flowing over the debris mass, can mix with the debris mass after initial failure and thus saturate the debris. When this happens, the slide can transform into a debris flow.

### 5. Conclusions

This study shows that in the TCP debris flow trigger zone debris flows probably start as landslides which quickly turn into debris flows as they move downslope. Furthermore, it shows that quantitative physical modelling of debris flow triggering often still suffers from shortcomings, which makes it hard to apply such an approach to practical problems. This is caused by two main factors:

Firstly, there is the variation in the values of the input parameters of the trigger model, resulting from natural variations and measurement errors. When applying this variation in input values to a trigger model, this results in a wide distribution of model output values. In this study, the relative uncertainty in model results is 3 times

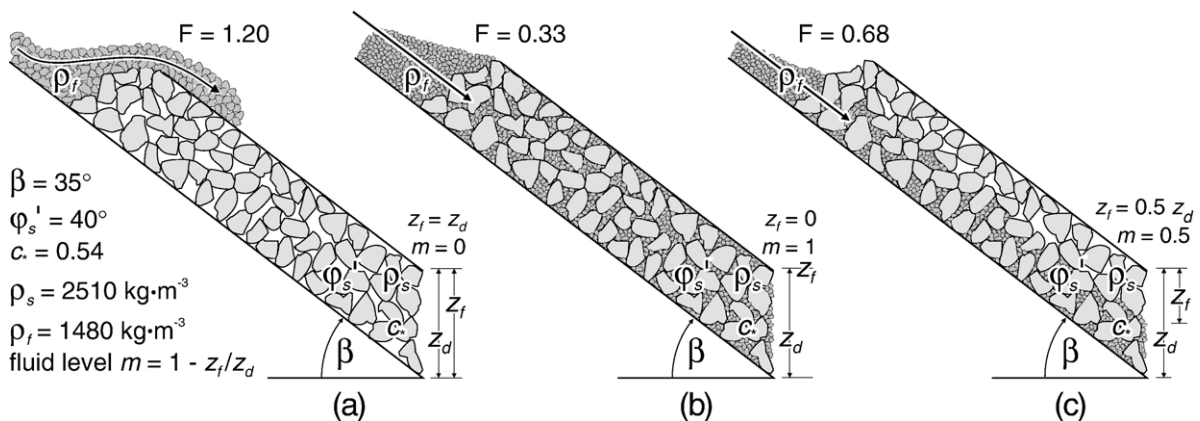


Fig. 5. Three typical situations if a rock–fluid mixture reaches an accumulation of coarse debris.

wider than in any of the input parameters. These variations however cannot explain the apparent stability in many situations as  $F$  in Fig. 3 stays far below 1.0.

This brings us to the second problem, the flow behaviour. There appears to be an upper bound for fluid flow through the pores of debris. With increasing stone content and stone size of the fluid there is a point where the stones in the fluid will block the pores; the fluid will then no longer flow through the pores, but it will start to run over the debris. This strongly influences the actual trigger mechanism of debris flows.

## 6. Symbols

$B$	Intrinsic viscosity [–]
$c_*$	Volumetric concentration of solids in static debris [–]
$c_s$	Volumetric solids content of debris [–]
$cv_V$	Coefficient of variation of stone volumes [–]
$d_{ch}$	Characteristic grain diameter [m]
$F$	Safety factor [–]
$g$	Gravity acceleration [ $m\ s^{-2}$ ]
$h_0$	Depth of water film at the surface [m]
$m_{b/a}$	Mean ratio of intermediate to major stone axis [–]
$y$	Depth [m]
$y_f$	Failure depth [m]
$\beta$	Slope angle [°]
$\varphi'_k$	Kinetic internal friction angle [°]
$\varphi'_s$	Effective static angle of internal friction [°]
$\kappa$	Constant $\approx 1$ [–]
$\eta_{if}$	Viscosity of interstitial fluid [ $kg\ m^{-1}\ s^{-1}$ ]
$\eta_N$	Newtonian viscosity [ $kg\ m^{-1}\ s^{-1}$ ]
$\rho_f$	Fluid density [ $kg\ m^{-3}$ ]
$\rho_s$	Solids density [ $kg\ m^{-3}$ ]
$\tau$	Shear stress [Pa]
$\tau_f$	Maximum shear resistance [Pa]
$\theta_s$	Porosity [–]

## Acknowledgements

I wish to thank Th.W.J. van Asch, Dr. H. Van Steijn and Prof. Dr. J.D. Nieuwenhuis for their contributions to this paper. Also, I am indebted to the laboratory staff and the students who participated in the field campaigns. Finally, I am grateful to the EU research programme EPOCH (European Programme on Climatology and Natural Hazards in the European Community) for funding a major part of the research.

## References

- Azimi, C., Desvarreux, P., 1974. A study of one special type of mudflow in the French Alps. *Quarterly Journal of Engineering Geology* 7, 329–338.
- Bagnold, R.A., 1954. Experiments on a gravity-free dispersion of large solid spheres in a Newtonian fluid under shear. *Proceedings of the Royal Society of London* 225A, 49–63.
- Bentley, S.P., 1979. Viscometric assessment of remoulded sensitive clays. *Canadian Geotechnical Journal* 16, 414–419.
- Berti, M., Genevois, R., Simoni, A., Tecca, P.R., 1999. Field observations of a debris flow event in the Dolomites. *Geomorphology* 29, 265–274.
- Blijenberg, H.M., 1995. In-situ strength tests of coarse, cohesionless debris on scree slopes. *Engineering Geology* 39, 137–146.
- Blijenberg, H.M., 1998. Rolling Stones? Triggering and frequency of hillslope debris flows in the Bachelard Valley, southern French Alps. KNAG/Faculteit Ruimtelijke Wetenschappen Universiteit Utrecht: Utrecht. Netherlands Geographical Studies 246. Also: PhD thesis, Utrecht University.
- Campbell, R.H., 1974. Debris flows originating from soil slips during rainstorms in southern California. *Quarterly Journal of Engineering Geology* 7, 339–349.
- Cannon, S.H., Kirkham, R.M., Parise, M., 2001. Wildfire-related debris-flow initiation processes, Storm King Mountain, Colorado. *Geomorphology* 39, 171–188.
- Charles, J.A., 1991. Laboratory shear strength tests and the stability of rockfill slopes. In: Das Neves, E.M. (Ed.), *Advances in Rockfill Structures*. Proceedings of the NATO Advanced Study Institute on Advances in Rockfill Structures. NATO ASI Series E: Applied Sciences, vol. 200. Kluwer, Dordrecht, pp. 53–72.
- Chen, C.L., 1986. Chinese concepts of modeling hyperconcentrated streamflow and debris flow. *Proceedings of the Third International Symposium on River Sedimentation*, Jackson, Mississippi 1647–1657.
- Chen, C.L., 1988. General solutions for viscoplastic debris flow. *Journal of Hydraulic Engineering* 114, 259–282.
- Costa, J.E., 1984. Physical geomorphology of debris flows. In: Costa, J.E., Fleisher, P.J. (Eds.), *Developments and Applications of Geomorphology*. Springer Verlag, Berlin/Heidelberg, pp. 268–317.
- Duzgun, H.S.B., Yucemen, M.S., Karpuz, C., 2002. A probabilistic model for the assessment of uncertainties in the shear strength of rock discontinuities. *International Journal of Rock Mechanics and Mining Sciences* 39, 743–754.
- European Commission, 1994. *Klimafaktoren und Natürliche Risiken im Alpenraum*. European Commission.
- Flageollet, J.C. (Ed.), 1993. *Temporal Occurrence and Forecasting of Landslides in the European Community*. Part I: Methodology (Reviews) for the Temporal Study of Landslides. Part II: Case Studies of the Temporal Occurrence of Landslides in the European Community.
- Fleming, R.W., Ellen, S.D., Albus, M.A., 1989. Transformation of dilative and contractive landslide debris into debris flows — an example from Marin County, California. *Engineering Geology* 27, 201–223.
- Gregoretti, G., 2000. Experimental evidence from the triggering of debris flow along a granular slope. *Physics and Chemistry of the Earth*. Part B: Hydrology, Oceans and Atmosphere 25 (4), 387–390.
- Haeberli, W., Rickenmann, D., Zimmermann, M., Rösli, U., 1990. Investigation of 1987 debris flows in the Swiss Alps: general concept and geophysical soundings. In: Sinniger, R.O., Monbaron, M. (Eds.), *Hydrology in Mountainous Regions*. Part II: Artificial Reservoirs; Water and Slopes. *Proceedings of the two Lausanne Symposia*, August 1990, vol. 194. IAHS Publications, pp. 303–310.

- Hungr, O., Morgenstern, N.R., 1984a. Experiments on the flow behaviour of granular materials at high velocity in an open channel flow. *Geotechnique* 34, 405–413.
- Hungr, O., Morgenstern, N.R., 1984b. High velocity ring shear tests on sand. *Geotechnique* 34, 415–421.
- Innes, J.L., 1985. Lichenometric dating of debris-flow deposits on alpine colluvial fans in southwest Norway. *Earth Surface Processes and Landforms* 10, 519–524.
- Iverson, R.M., Reid, M.E., Lahusen, R.G., 1997. Debris-flow mobilization from landslides. *Annual Review of Earth and Planetary Science* 25, 85–138.
- Johnson, A.M., Rahn, P.H., 1970. Mobilization of debris flows. In: Macar, P. (Ed.), *New Contributions to Slope Evolution Zeitschrift für Geomorphologie Neue Folge Supplementband*, vol. 9, pp. 168–186.
- Kenney, C., 1984. Properties and behaviours of soils relevant to slope instability. In: Brunsden, D., Prior, D.B. (Eds.), *Slope Instability*. Wiley, London, pp. 27–65.
- Kobashi, S., Suzuki, M., 1987. The critical rainfall (danger index) for disasters caused by debris flows and slope failures. In: Beschta, R.L., et al. (Ed.), *Erosion and Sedimentation in the Pacific Rim. Proceedings of the Corvallis Symposium, August 1987*, vol. 165. IAHS Publications, pp. 201–211.
- Kotarba, A., 1989. On the age of debris flows in the Tatra Mountains. *Studia Geomorphologica Carpatho-Balcanica* 23, 139–152.
- Kotarba, A., 1997. Formation of high-mountain talus slopes related to debris-flow activity in the High-Tatra Mountains. *Permafrost and Periglacial Processes* 8, 191–204.
- Lahousse, P., Salvador, P.-G., 1998. La crue torrentielle du Bez (Hautes-Alpes, Briançonnais), 24 juillet 1995. *Geodinamica Acta* 11, 163–170.
- Lambe, T.W., Whitman, R.V., 1969. *Soil Mechanics*. Wiley, New York.
- Lin, M.L., Jeng, F.S., 2000. Characteristics of hazards induced by extremely heavy rainfall in Central Taiwan—Typhoon Herb. *Engineering Geology* 58, 191–207.
- Martinez, J.M., Avila, G., Agudelo, A., Schuster, R.L., Casadevall, T.J., Scott, K.M., 1995. Landslides and debris flows triggered by the 6 June 1994 Paez earthquake, southwestern Colombia. *Landslide News* 9, 13–15.
- Martins, R., 1991. Principles of rockfill hydraulics. In: Das Neves, E.M. (Ed.), *Advances in Rockfill Structures. Proceedings of the NATO Advanced Study Institute on Advances in Rockfill Structures*. NATO ASI Series E: Applied Sciences, vol. 200. Kluwer, Dordrecht, pp. 523–570.
- Mathys, N., Brochot, S., Meunier, M., Richard, D., 2003. Erosion quantification in the small marly experimental catchments of Draix (Alpes de Haute Provence, France). Calibration of the ETC rainfall—runoff-erosion model. *Catena* 50, 527–548.
- Ocakuglu, F., Gokceoglu, C., Ercanoglu, M., 2002. Dynamics of a complex mass movement triggered by heavy rainfall: a case study from NW Turkey. *Geomorphology* 42, 329–341.
- Okunishi, K., Suwa, H., Hamana, S., 1988. Hydrological controls of erosion and sediment transport in volcanic torrents. *Hydrological Sciences Journal/Journal des Sciences Hydrologiques* 33, 575–587.
- Oostwoud Wijdenes, D.J., Ergenzinger, P., 2003. Erosion and sediment transport on steep marly hillslopes, Draix, Haute-Provence, France: an experimental field study. *Catena* 33, 179–200.
- Pierson, T.C., 1981. Dominant particle support mechanisms in debris flows at Mt. Thomas, New Zealand, and implications for flow mobility. *Sedimentology* 28, 49–60.
- Sassa, K., 1985. The mechanics of debris flow. *Proceedings of the 11th International Conference on Soil Mechanics and Foundation Engineering*, vol. 3, pp. 1173–1176.
- Sassa, K., Fukuoka, H., Wang, F., 1997. Gamahara Torrent debris flow on 6 December 1996, Japan. 2. Possible mechanism of the debris flow. *Landslide News* 10, 6–9.
- Statham, I., 1977. *Earth Surface Sediment Transport*. Clarendon Press, Oxford, 178 pp.
- Strunk, H., 1991. Frequency distribution of debris flows in the Alps since the ‘Little Ice Age’. In: De Ploey, J., Haase, G., Leser, H. (Eds.), *Geomorphology and Geoecology. V. Geomorphological Approaches in Applied Geography. Proc. 2nd Int. Conf. Geom., Frankfurt/Main, 1989 Zeitschrift für Geomorphologie Neue Folge Supplementband*, vol. 83, pp. 71–81.
- Takahashi, T., 1978. Mechanical characteristics of debris flow. *Journal of the Hydraulic Division, Proceedings ASCE 104 HY8, Proceedings Paper, 13971*, pp. 1153–1169.
- Takahashi, T., 1980. Debris flow on prismatic open channel. *Proceedings ASCE 106 HY3, proceedings paper 15245. Journal of the Hydraulics Division*, pp. 381–396.
- Takahashi, T., 1981. Estimation of potential debris flows and their hazardous zones; soft countermeasures for a disaster. *Journal of Natural Disaster Science* 3, 57–89.
- Takahashi, T., Ashida, K., Sawai, K., 1981. Delineation of debris flow hazard areas. *Erosion and Sedimentation in Pacific Rim Steep-lands. Proceedings of the Christchurch Symposium, January 1981*, vol. 132. IAHS Publications, pp. 589–603.
- Takahashi, T., Nakagawa, H., Harada, T., Yamashiki, Y., 1992. Routing debris flows with particle segregation. *Journal of Hydraulic Engineering* 118, 1490–1507.
- Van Asch, T.H.W.J., Van Steijn, H., 1991. Temporal patterns of mass movements in the French Alps. *Catena* 18, 515–527.
- Van Steijn, H., Coutard, J.-P., 1989. Laboratory experiments with small debris flows: physical properties related to sedimentary characteristics. *Earth Surface Processes and Landforms* 14, 587–596.
- Varnes, D.J., 1978. Slope movement types and processes. In: Schuster, R.L., Krizek, R.J. (Eds.), *Landslides, Analysis and Control*, Washington Transportation Research Board of the National Academy of Sciences special report, vol. 176, pp. 11–33.
- Villi, V., Dal Pra, A., 2002. Debris flow in the upper Isarco valley, Italy — 14 August 1998. *Bulletin of Engineering Geology and the Environment* 61, 49–57.
- Zimmermann, M., 1990. Debris flows 1987 in Switzerland: geomorphological and meteorological aspects. In: Sinniger, R.O., Monbaron, M. (Eds.), *Hydrology in Mountainous Regions. Part II: Artificial Reservoirs; Water and Slopes. Proceedings of the two Lausanne Symposia, August 1990*, vol. 194. IAHS Publications, pp. 387–393.